High-Relaxivity Gd(III)–Hemicryptophane Complex

Estelle Godart, Augustin Long, Roselyne Rosas, Gilles Lemercier, Marion Jean, Sebastien Leclerc, Sabine Bouguet-Bonnet, Célia Godfrin, Laure-Lise Chapellet, Jean-Pierre Dutasta, et al.

High-Relaxivity Gd(III)−Hemicryptophane Complex

Godart, E.
Long, A.
Rosas, R.
Lemercier, G.
Jean, M.
Leclerc, S.
Bouguet-Bonnet, S.
Godfrin, C.
Chapellet, L. L.
Dutasta, J. P.
Martinez, A.

ABSTRACT: The polytopic hemicryptophane cage **HC1** combining a cyclotriveratrylene (CTV) unit and a tris(2-aminoethyl)amine (tren) moiety connected by three 2-hydroxyisophthalamide linkers was synthesized in 12 steps. The resulting highly functionalized covalent host is soluble in aqueous medium and has been used to complex Gd(III) ion. The Gd(III)@**HC1** complex presents promising relaxivity properties when compared to the clinically used Dotarem MRI agent.

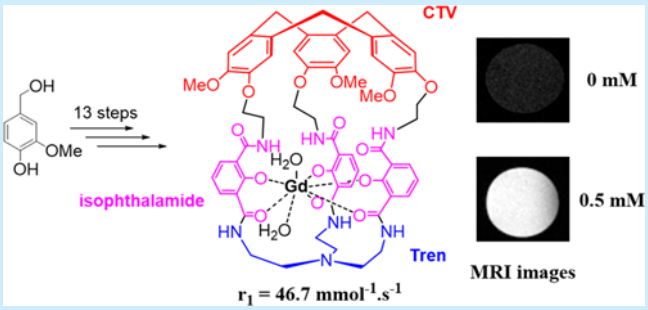

Synthetic cage molecules arise a considerable interest because of their ability to mimic the remarkable properties of enzymes.[1−17] Among the covalent cages based on cyclodextrins, calixarenes, pillararenes and cavitands, hemicryptophanes and cryptophanes are two classes of molecular containers built from the cyclotriveratrylene (CTV) unit.[18,19] The cryptophanes,[19,20] consisting of two CTV units, display remarkable recognition properties toward small neutral molecules (epoxydes, CHBrClF),[21] metal ions (Cs^+),[22] and noble gas (xenon, radon).[23] The hemicryptophanes, which combine a CTV moiety with another C_3 symmetrical unit (respectively designated as north and south parts), have found applications in molecular recognition or can act as molecular machines or supramolecular catalysts.[19] Numerous and various interactions are involved in the formation of the guest−hemicryptophane complexes because of their heteroditopic character. As a consequence and depending on the size and shape of their cavity, hemicryptophanes are able to recognize selectively various substrates ranging from single cations or ion pairs to chiral neurotransmitters and carbohydrates.[24,25] On the other hand, these host compounds can bind phosphorus or transition metals ions like V(V), Zn(II), Co(II), and Cu(II) in the heart of their cavity leading to endohedral functionalized molecular cages, which have been used as supramolecular catalysts.[26]

Most of the hemicryptophanes synthesized so far differ by the C_3-symmetry moiety facing the CTV unit and by the nature of the linkers between the CTV and the second C_3 unit. Functionalized groups have been introduced in the structure of cryptophanes leading to original hosts presenting for instance remarkable complexation properties toward lanthanide cations.[27] Such a strategy has been scarcely used for hemicryptophane derivatives, although it should be of great interest for the design of original receptors with applications in supramolecular catalysis or in developing new coordination complexes of transition metals. It is with that perspective that we designed and synthesized the new hemicryptophane **HC1** bearing 2-hydroxyisophthalamide moieties in the linkers. The polytopic hemicryptophane **HC1** was found to be water-soluble in basic media and suitable for complexing f-transition metal cations. To explore this potentiality, the Gd^{3+}@**HC1** complex was prepared and its T_1-relaxation properties were investigated, showing a longitudinal relaxivity about three times higher than that of the commercial DOTA complex (DOTA for 1,4,7,10-tetraazacyclododecane-1,4,7,10-tetra-acetate).

Three main methods are used to synthesize hemicryptophanes: (i) the [1 + 1] coupling between the south unit and the CTV moiety, (ii) the cage-closing reaction at the south part from an adequate CTV precursor, and (iii) the cage-closing reaction of the north part to form the CTV unit from an appropriately substituted south moiety. The third method was applied for the synthesis of hemicryptophane **HC1**

(Schemes 1−3). This approach has proved to be successful for the synthesis of hemicryptophanes bearing a triamido-amine

Scheme 1. Synthesis of Intermediate 5

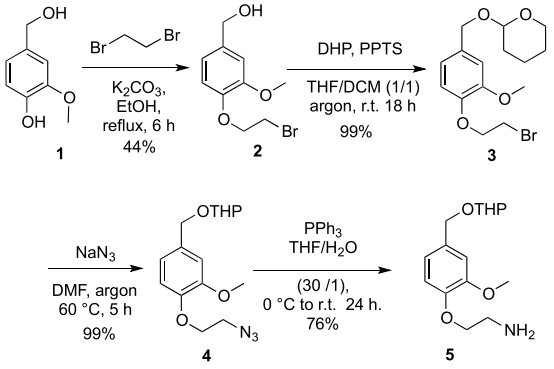

group in their south part. Starting from vanillyl alcohol **1**, compound **2** was obtained in 44% yield by alkylation of the phenol unit with dibromoethane. The subsequent protection by a DHP group afforded compound **3**. The next step consists of a quantitative nucleophilic substitution of bromine by sodium azide (compound **4**) followed by a Staudinger reduction that provides the amino intermediate **5** in 33% overall yield (Scheme 1).

We then chose to protect the hydroxy group of the 2-hydroxyisophthalic acid by an allyl group in order (i) to avoid the concomitant location of amine and phenol on various intermediates, which should lead to zwitterionic species probably difficult to purify and (ii) to deprotect it easily and orthogonally to the methyl ether located on the CTV unit. The demethylation of the commercially available 2-methoxyisophthalic acid **6**, under strong acidic conditions, gave the 2-hydroxyisophthalic acid **7**, which was then heated in the presence of a base and allyl bromide to afford **8** in 69% yield. The saponification of the ester functions provided the desired product **9** (Scheme 2).[28]

Scheme 2. Synthesis of Intermediate 9: (a) HBr/AcOH (1:1), 90 °C, 45 min. (b) Allyl bromide (5 equiv), K_2CO_3 (10 equiv), argon, DMF, 75 °C, 20 h. (c) NaOH (3 equiv), MeOH/H_2O 1/1, r.t. 48 h

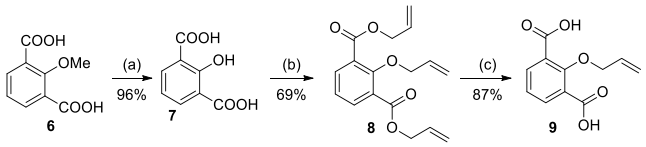

The diacid **9** was converted to the diacyl chloride, which reacted with 2 equiv of mercaptothiazoline to form the intermediate **10** (Scheme 3). Then, **11** was prepared by adding dropwise a default of compound **5** in a diluted solution of **10** in dichloromethane in order to graft only 1 equiv of the amine **5**. After separation by chromatography, the excess of reactant **10** was recovered and the reaction started again several times until a good yield for the formation of intermediate **11** was reached (80%). Reaction of **11** with the tris(2-aminoethyl)amine (tren) in CH_2Cl_2 (DCM) at room temperature provided the precursor of cyclization **12** in 88% yield. The macrocyclization was then performed using formic acid as solvent under moderate dilution condition (10^{-3} M); the expected hemi-

Scheme 3. Synthesis of Hemicryptophane HC1[a]

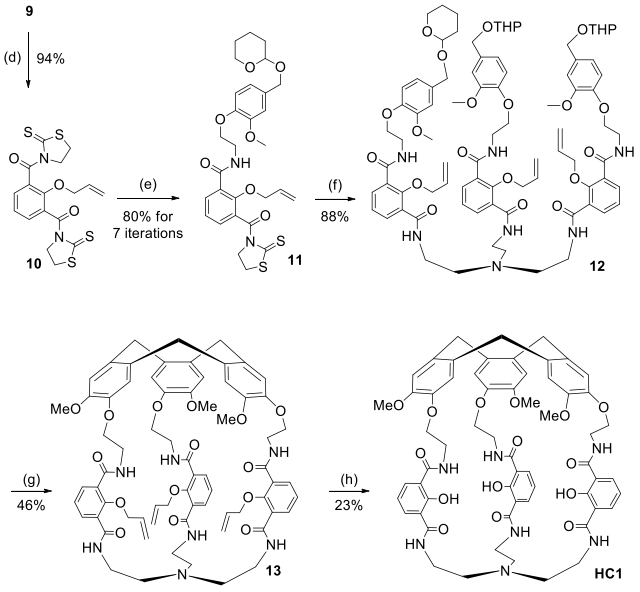

[a](d) (1) $C_2O_2Cl_2$ (2.4 equiv), DMF, argon, dioxane, 60 °C, 17 h; (2) NEt_3 (2.5 equiv), mercaptothiazoline (2.4 equiv), THF 0 °C to r.t. 15 h. (e) **5** (0.15 equiv) added dropwise during 10 h under stirring, DCM, r.t. (f) Tren (tris(2-aminoethyl)amine) (0.3 equiv), DCM, r.t. 15 h. (g) HCOOH, $CHCl_3$ (traces) 30 °C, 48 h. (h) $Pd(PPh_3)_4$ (0.1 equiv), K_2CO_3 (10 equiv), DCM/MeOH 1/1, argon, r.t. 36 h.

cryptophane **13** was obtained in a relatively good yield (46%). This is consistent with our previous observation related to the formation of hemicryptophane presenting triamido-amine in their south part, suggesting the preorganization of the precursor of cyclization in formic acid by complexation of a proton by the triamido-amine moiety.[29] Finally, the allyl protecting groups were removed using tetrakis-(triphenylphosphine)-palladium(0) under basic conditions. The steric hindrance imposed by the cavity around the protected phenols and the difficulty related to the purification of such functionalized cage could account for the relative low yield of the deprotection step (23%). Following this 12-step synthesis, hemicryprophane **HC1** was obtained with an overall yield of 1.5%.

The ^{1}H NMR spectrum of hemicryptophane **HC1** displayed in Figure 1 shows that the structure is on average of C_3 symmetry in solution. The expected signals of the CTV moieties can be observed: (i) the AB systems for the $ArCH_2$ bridges of the CTV units appear as two doublets at 3.51 ppm and 4.66, (ii) the methoxy groups at 3.67 ppm, and (iii) two singlets for the aromatic protons at 7.02 and 7.08 ppm. The CH_2 protons of the lower part exhibit chemical shifts at 3.52 and 2.62 ppm. The aromatic protons of the linkers in meta- and para-position to the oxygen atom display two doublets between 7.88 and 8.11 ppm and a triplet at 6.62 ppm, respectively. The diastereotopic aliphatic protons of the linkers show broad multiplets between 3.6 and 4.3 ppm. It can be noted that host **HC1** is soluble in basic water (pH ≈10), making it one of the rare examples of water-soluble hemicryptophanes.[30]

The multiple coordination sites in hemicryptophane **HC1** are particularly suited for the binding of f-transition metals, and the endohedral functionalization of the host molecule should favor the complexation of the metal ion inside the molecular

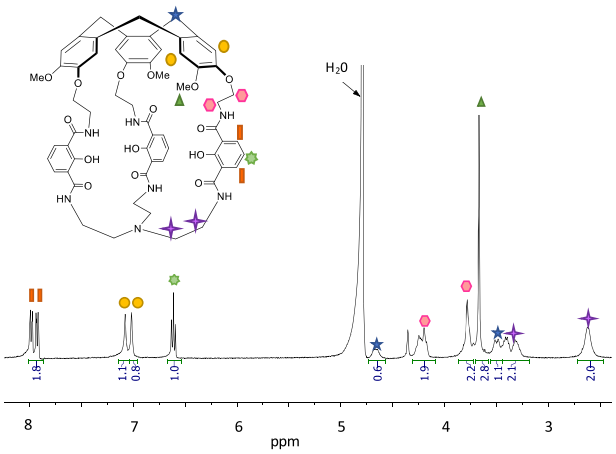

Figure 1. ^{1}H NMR spectra of hemicryptophane **HC1** in basic D_2O.

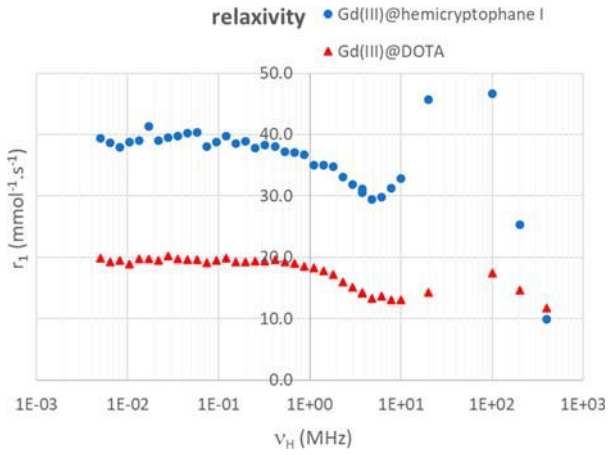

Figure 2. Comparison of water ^{1}H relaxivities as a function of the ^{1}H Larmor frequency for solutions of Gd(III)@hemicryptophane **HC1** (blue circles) and Gd(III)@DOTA (red triangles). Solvent: 70/30 DMSO-d_6/H_2O; T = 297 K.

cavity. The complexation of the strongly paramagnetic Gd(III) ion is of particular interest as the resulting complex could be used as MRI contrast agent like, for instance, Gd(III)−DOTA, Gd(III)−DTPA complexes,[31] pyridine-based chelates with two hydrazine functions,[32b] or tris-hydroxypyridonate Gd(III) complexes.[32] Moreover, it was recently shown that confinement of Gd(III) complexes into nanosystems such as silica nanoparticules, zeolites, apoferritine, and hydrogels improved their relaxivity r_1.[33] This prompted us to investigate if the confinement of Gd(III) in the heart of molecular cage could lead to similar effects.

The Gd(III)@**HC1** complex was obtained by stirring overnight 1 equiv of ligand with 1 equiv of $Gd(OTf)_3$ in methanol in the presence of an excess of NEt_3 at 60 °C (Scheme S1). The mass spectrum of Gd(III)@**HC1** suggests that, at least, one water molecule is coordinated to the Gd(III) metal center (Figure S26). We then explored more accurately the NMR relaxation properties of the new complex for a potential use as an MRI contrast agent. First, longitudinal relaxation times T_1 were measured: solutions of Gd(III)@**HC1** in DMSO-d_6/water (70/30) at different concentrations were prepared, and for each one the water proton T_1 was measured as a function of the magnetic field values (or equivalently of the ^{1}H Larmor frequency). The longitudinal relaxivity r_1 is obtained by normalizing the relaxation enhancement of water protons to a millimolar solution of the chelated Gd(III) (Figure 2).[34] It characterizes the contribution of the paramagnetic ion to the acceleration of water protons' relaxation rate $1/T_1$. A longitudinal relaxivity of 46.7 $mmol^{-1}$ s^{-1} was obtained for Gd(III)@**HC1** at a 2.35 T magnetic field (100 MHz ^{1}H Larmor frequency) at 297 K. As the viscosity of the solution can influence the relaxation parameters, we measured the relaxivity of Dotarem Gd(III)−DOTA in the same 70/30 DMSO-d_6/H_2O mixture at the same temperature. The relaxivity of Dotarem under these conditions is 2.7 times lower than that of the hemicryptophane complex (r_1(Dotarem, 100 MHz) = 17.48 $mmol^{-1}$ s^{-1}). Thus, a much better relaxivity of the encaged complex is observed in the frequency zone of interest for medical imaging (64−128 MHz). This higher relaxivity can be attributed to three main factors: (i) a higher number of inner-sphere water molecules, (ii) an improvement of rate of exchange of these water molecules with bulk solution, and (iii) a decrease of the tumbling rate of the complex.[31]

Contrast agents allow an enhancement of image contrast by lowering the relaxation time of water protons in the tissues when they are present. Figure 3 shows MRI images obtained

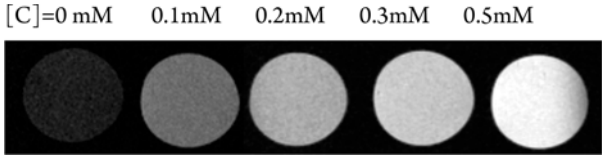

Figure 3. T_1-weighted MRI images of 4 hemicryptophane−Gd(III) solutions with the following concentrations (from left to right): 0 mM, 0.1 mM, 0.2 mM, 0.3 mM, and 0.5 mM. Solvent: 70/30 DMSO-d_6/H_2O.

with Gd(III)@**HC1** hemicryptophane complex. Images were recorded at 2.34 T with phantoms corresponding to different concentrations of the Gd(III)@**HC1** hemicryptophane complex. They were obtained with a T_1 weighting (Figure 3). As expected, an increase of the signal with the complex concentration is observed in T_1-weighted images, revealing that the Gd(III)@**HC1** acts as an efficient contrast agent. This cage structure reveals thus promising since it gives efficient MRI agent presenting improved longitudinal relaxivity when compared to commercial ones.

In summary, we have described the synthesis of the highly functionalized hemicryptophane cage **HC1**, where the southern part, bearing an amine function, is connected to the CTV northern part by three linkers, each including the 2-hydroxyisophthalamide moiety. This cage ligand was used to encapsulate gadolinium(III) ion inside its cavity. The resulting complex exhibits a remarkable longitudinal relaxivity of 46.7 $mmol^{-1}$ s^{-1} (at 100 MHz), 2.7 times higher than the commercial Dotarem MRI agent under the same conditions. This complexation of a f-transition metal in a hemicryptophane cavity is, to our knowledge, unprecedented and opens up the way for a larger use of this class of host molecules as ligand for other f-transition metal ions and wider applications in fluorescence or circularly polarized luminescence (CPL) for instance (see Figures S30−S32 for the chiral HPLC resolution of hemicryptophane **13**).

(1) Sanders, J. K. M. Supramolecular Catalysis in Transition. *Chem. - Eur. J.* **1998**, *4*, 1378−1383.
(2) Lehn, J.-M. Supramolecular Chemistry: From Molecular Information towards Self-Organization and Complex Matter. *Rep. Prog. Phys.* **2004**, *67*, 249.
(3) Steed, J. W.; Atwood, J. L. *Supramolecular Chemistry*, 2nd ed.; Wiley-Blackwell, 2009.
(4) Raynal, M.; Ballester, P.; Vidal-Ferran, A.; van Leeuwen, P. W. N. M. Supramolecular Catalysis. Part 1: Non-Covalent Interactions as a Tool for Building and Modifying Homogeneous Catalysts. *Chem. Soc. Rev.* **2014**, *43*, 1660−1733.
(5) Raynal, M.; Ballester, P.; Vidal-Ferran, A.; van Leeuwen, P. W. N. M. Supramolecular Catalysis. Part 2: Artificial Enzyme Mimics. *Chem. Soc. Rev.* **2014**, *43*, 1734−1787.
(6) Rebek, J. Molecular Behavior in Small Spaces. *Acc. Chem. Res.* **2009**, *42*, 1660−1668.
(7) Yoshizawa, M.; Klosterman, J. K.; Fujita, M. Functional Molecular Flasks: New Properties and Reactions within Discrete, Self-Assembled Hosts. *Angew. Chem., Int. Ed.* **2009**, *48*, 3418−3438.
(8) Leenders, S. H. A. M.; Gramage-Doria, R.; de Bruin, B.; Reek, J. N. H. Transition Metal Catalysis in Confined Spaces. *Chem. Soc. Rev.* **2015**, *44*, 433−448.
(9) Feiters, M. C.; Rowan, A. E.; Nolte, R. J. M. From Simple to Supramolecular Cytochrome P450 Mimics. *Chem. Soc. Rev.* **2000**, *29*, 375−384.
(10) Hong, C. M.; Bergman, R. G.; Raymond, K. N.; Toste, F. D. Self-Assembled Tetrahedral Hosts as Supramolecular Catalysts. *Acc. Chem. Res.* **2018**, *51*, 2447−2455.
(11) Wiester, M. J.; Ulmann, P. A.; Mirkin, C. A. Enzyme Mimics Based Upon Supramolecular Coordination Chemistry. *Angew. Chem., Int. Ed.* **2011**, *50*, 114−137.
(12) Chambron, J.-C.; Meyer, M. The Ins and Outs of Proton Complexation. *Chem. Soc. Rev.* **2009**, *38*, 1663−1673.
(13) Isaacs, L. Stimuli Responsive Systems Constructed Using Cucurbit[n]uril-Type Molecular Containers. *Acc. Chem. Res.* **2014**, *47*, 2052−2062.
(14) Ghale, G.; Nau, W. M. Dynamically Analyte-Responsive Macrocyclic Host−Fluorophore Systems. *Acc. Chem. Res.* **2014**, *47*, 2150−2159.
(15) Hargrove, A. E.; Nieto, S.; Zhang, T.; Sessler, J. L.; Anslyn, E. V. Artificial Receptors for the Recognition of Phosphorylated Molecules. *Chem. Rev.* **2011**, *111*, 6603−6782.
(16) Park, J. S.; Sessler, J. L. Tetrathiafulvalene (TTF)-Annulated Calix[4]pyrroles: Chemically Switchable Systems with Encodable Allosteric Recognition and Logic Gate Functions. *Acc. Chem. Res.* **2018**, *51*, 2400−2410.
(17) Zhang, D.; Ronson, T. K.; Nitschke, J. R. Functional Capsules via Subcomponent Self-Assembly. *Acc. Chem. Res.* **2018**, *51*, 2423−2436.
(18) (a) El-Ayle, G.; Holman, K. T. Cryptophanes. In *Comprehensive Supramolecular Chemistry II*; Atwood, J. L., Gokel, G. W., Barbour, L. J., Eds.; Elsevier: New York, 2017. (b) Hardie, M. J. Self-Assembled Cages and Capsules Using Cyclotriveratrylene-Type Scaffolds. *Chem. Lett.* **2016**, *45*, 1336−1346. (c) Henkelis, J. J.; Hardie, M. J. Controlling the Assembly of Cyclotriveratrylene-Derived Coordination Cages. *Chem. Commun.* **2015**, *51*, 11929−11943. (d) Brotin, T.; Dutasta, J.-P. Cryptophanes and Their Complexes—Present and Future. *Chem. Rev.* **2009**, *109*, 88−130.
(19) (a) Zhang, D.; Martinez, A.; Dutasta, J.-P. Emergence of Hemicryptophanes: From Synthesis to Applications for Recognition, Molecular Machines, and Supramolecular Catalysis. *Chem. Rev.* **2017**, *117*, 4900−4942. (b) Canceill, J.; Collet, A.; Gabard, J.; Kotzyba-Hibert, F.; Lehn, J.-M. Speleands. Macropolycyclic Receptor Cages Based on Binding and Shaping Sub-Units. Synthesis and Properties of Macrocycle Cyclotriveratrylene Combinations. Preliminary Communication. *Helv. Chim. Acta* **1982**, *65*, 1894−1897.
(20) (a) Brégier, F.; Hudeček, O.; Chaux, F.; Penouilh, M.-J.; Chambron, J.-C.; Lhoták, P.; Aubert, E.; Espinosa, E. Generation of Cryptophanes in Water by Disulfide Bridge Formation. *Eur. J. Org. Chem.* **2017**, *2017*, 3795−3811. (b) Kai, S.; Kojima, T.; Thorp-Greenwood, F. L.; Hardie, M. J.; Hiraoka, S. How Does Chiral Self-Sorting Take Place in the Formation of Homochiral Pd_6L_8 Capsules Consisting of Cyclotriveratrylene-Based Chiral Tritopic Ligands? *Chem. Sci.* **2018**, *9*, 4104−4108. (c) Dubost, E.; Kotera, N.; Garcia-Argote, S.; Boulard, Y.; Léonce, E.; Boutin, C.; Berthault, P.; Dugave, C.; Rousseau, B. Synthesis of a Functionalizable Water-Soluble Cryptophane-111. *Org. Lett.* **2013**, *15*, 2866−2868.
(21) (a) Bouchet, A.; Brotin, T.; Linares, M.; Ågren, H.; Cavagnat, D.; Buffeteau, T. Enantioselective Complexation of Chiral Propylene Oxide by an Enantiopure Water-Soluble Cryptophane. *J. Org. Chem.* **2011**, *76*, 4178−4181. (b) Canceill, J.; Lacombe, L.; Collet, A. Analytical optical resolution of bromochlorofluoromethane by enantioselective inclusion into a tailor-made cryptophane and determination of its maximum rotation. *J. Am. Chem. Soc.* **1985**, *107*, 6993−6996.
(22) (a) Brotin, T.; Cavagnat, D.; Berthault, P.; Montserret, R.; Buffeteau, T. Water-Soluble Molecular Capsule for the Complexation of Cesium and Thallium Cations. *J. Phys. Chem. B* **2012**, *116* (35), 10905−10914. (b) Brotin, T.; Montserret, R.; Bouchet, A.; Cavagnat, D.; Linares, M.; Buffeteau, T. High Affinity of Water-Soluble Cryptophanes for Cesium Cations. *J. Org. Chem.* **2012**, *77* (2), 1198−1201.
(23) (a) Fairchild, R. M.; Joseph, A. I.; Holman, K. T.; Fogarty, H. A.; Brotin, T.; Dutasta, J.-P.; Boutin, C.; Huber, G.; Berthault, P. A Water-Soluble Xe@cryptophane-111 Complex Exhibits Very High Thermodynamic Stability and a Peculiar ^{129}Xe NMR Chemical Shift. *J. Am. Chem. Soc.* **2010**, *132*, 15505−15507. (b) Joseph, A. I.; Lapidus, S. H.; Kane, C. M.; Holman, K. T. Extreme Confinement of Xenon by Cryptophane-111 in the Solid State. *Angew. Chem., Int. Ed.* **2015**, *54*, 1471−1475. (c) Taratula, O.; Bai, Y.; D'Antonio, E. L.; Dmochowski, I. J. Enantiopure Cryptophane-^{129}Xe Nuclear Magnetic Resonance Biosensors Targeting Carbonic Anhydrase. *Supramol. Chem.* **2015**, *27*, 65−71. (d) Tassali, N.; Kotera, N.; Boutin, C.; Léonce, E.; Boulard, Y.; Rousseau, B.; Dubost, E.; Taran, F.; Brotin, T.; Dutasta, J.-P.; et al. Smart Detection of Toxic Metal Ions, Pb^{2+} and Cd^{2+}, Using a ^{129}Xe NMR-Based Sensor. *Anal. Chem.* **2014**, *86*, 1783−1788. (e) Schröder, L.; Lowery, T. J.; Hilty, C.; Wemmer, D. E.; Pines, A. Molecular Imaging Using a Targeted Magnetic Resonance Hyperpolarized Biosensor. *Science* **2006**, *314*, 446−449. (f) Riggle, B. A.; Wang, Y.; Dmochowski, I. J. A "Smart" ^{129}Xe NMR Biosensor for PH-Dependent Cell Labeling. *J. Am. Chem. Soc.* **2015**, *137*, 5542−5548. (g) Rose, H. M.; Witte, C.; Rossella, F.; Klippel, S.; Freund, C.; Schröder, L. Development of an Antibody-Based, Modular Biosensor for ^{129}Xe NMR Molecular Imaging of Cells at Nanomolar Concentrations. *Proc. Natl. Acad. Sci. U. S. A.* **2014**, *111*, 11697−

11702. (h) Khan, N. S.; Riggle, B. A.; Seward, G. K.; Bai, Y.; Dmochowski, I. J. Cryptophane-Folate Biosensor for ^{129}Xe NMR. *Bioconjugate Chem.* **2015**, *26*, 101−109. (i) Kotera, N.; Tassali, N.; Léonce, E.; Boutin, C.; Berthault, P.; Brotin, T.; Dutasta, J.-P.; Delacour, L.; Traoré, T.; Buisson, D.-A.; Taran, F.; Coudert, S.; Rousseau, B. A Sensitive Zinc-Activated ^{129}Xe MRI Probe. *Angew. Chem., Int. Ed.* **2012**, *51*, 4100−4103.

(24) (a) Perraud, O.; Robert, V.; Gornitzka, H.; Martinez, A.; Dutasta, J.-P. Combined Cation−π and Anion−π Interactions for Zwitterion Recognition. *Angew. Chem., Int. Ed.* **2012**, *51*, 504−508. (c) Cochrane, J. R.; Schmitt, A.; Wille, U.; Hutton, C. A. Synthesis of Cyclic Peptide Hemicryptophanes: Enantioselective Recognition of a Chiral Zwitterionic Guest. *Chem. Commun.* **2013**, *49*, 8504−8506. (d) Schmitt, A.; Chatelet, B.; Collin, S.; Dutasta, J.-P.; Martinez, A. Chiral Discrimination of Ammonium Neurotransmitters by C_3-Symmetric Enantiopure Hemicryptophane Hosts. *Chirality* **2013**, *25*, 475−479. (e) Makita, Y.; Katayama, N.; Lee, H.-H.; Abe, T.; Sogawa, K.; Nomoto, A.; Fujiwara, S.-I.; Ogawa, A. A Tri-Aromatic Amide Hemicryptophane Host: Synthesis and Acetylcholine Binding. *Tetrahedron Lett.* **2016**, *57*, 5112−5115.

(25) (a) Perraud, O.; Martinez, A.; Dutasta, J.-P. Exclusive Enantioselective Recognition of Glucopyranosides by Inherently Chiral Hemicryptophanes. *Chem. Commun.* **2011**, *47*, 5861−5863. (b) Long, A.; Perraud, O.; Albalat, M.; Robert, V.; Dutasta, J.-P.; Martinez, A. Helical Chirality Induces a Substrate-Selectivity Switch in Carbohydrates Recognitions. *J. Org. Chem.* **2018**, *83*, 6301−6306. (c) Zhang, D.; Mulatier, J.-C.; Cochrane, J. R.; Guy, L.; Gao, G. H.; Dutasta, J.-P.; Martinez, A. Helical, Axial, and Central Chirality Combined in a Single Cage: Synthesis, Absolute Configuration, and Recognition Properties. *Chem. - Eur. J.* **2016**, *22*, 8038−8042.

(26) (a) Martinez, A.; Dutasta, J.-P. Hemicryptophane−Oxidovanadium(V) Complexes: Lead of a New Class of Efficient Supramolecular Catalysts. *J. Catal.* **2009**, *267*, 188−192. (b) Zhang, D.; Jamieson, K.; Guy, L.; Gao, G.; Dutasta, J.-P.; Martinez, A. Tailored Oxido-Vanadium(V) Cage Complexes for Selective Sulfoxidation in Confined Spaces. *Chem. Sci.* **2017**, *8*, 789−794. (c) Makita, Y.; Sugimoto, K.; Furuyoshi, K.; Ikeda, K.; Fujiwara, S.; Shin-ike, T.; Ogawa, A. A Zinc(II)-Included Hemicryptophane: Facile Synthesis, Characterization, and Catalytic Activity. *Inorg. Chem.* **2010**, *49*, 7220−7222. (d) Makita, Y.; Ikeda, K.; Sugimoto, K.; Fujita, T.; Danno, T.; Bobuatong, K.; Ehara, M.; Fujiwara, S.; Ogawa, A. Enhancement of Catalytic Reactivity of Zinc(II) Complex by a Cyclotriveratrylene-Capped Structure. *J. Organomet. Chem.* **2012**, *706*−*707*, 26−29. (e) Perraud, O.; Sorokin, A. B.; Dutasta, J.-P.; Martinez, A. Oxidation of Cycloalkanes by H_2O_2 Using a Copper−Hemicryptophane Complex as a Catalyst. *Chem. Commun.* **2013**, *49*, 1288−1290. (f) Makita, Y.; Danno, T.; Ikeda, K.; Lee, H.-H.; Abe, T.; Sogawa, K.; Nomoto, A.; Fujiwara, S.-I.; Ogawa, A. Synthesis and Characterization of a Biphenyl-Linked Hemicryptophane and an Endohedral Cobalt-(II) Complex. *Tetrahedron Lett.* **2017**, *58*, 4507−4509.

(27) Roesky, C. E. O.; Weber, E.; Rambusch, T.; Stephan, H.; Gloe, K.; Czugler, M. A New Cryptophane Receptor Featuring Three Endo-Carboxylic Acid Groups: Synthesis, Host Behavior and Structural Study. *Chem. - Eur. J.* **2003**, *9*, 1104−1112.

(28) Samuel, A. P. S.; Moore, E. G.; Melchior, M.; Xu, J.; Raymond, K. N. Water-Soluble 2-Hydroxyisophthalamides for Sensitization of Lanthanide Luminescence. *Inorg. Chem.* **2008**, *47*, 7535−7544.

(29) Raytchev, P. D.; Perraud, O.; Aronica, C.; Martinez, A.; Dutasta, J.-P. A New Class of C_3-Symmetrical Hemicryptophane Hosts: Triamide- and Tren-Hemicryptophanes. *J. Org. Chem.* **2010**, *75*, 2099−2102.

(30) Brotin, T.; Martinez, A.; Dutasta, J.-P. Water-Soluble Cryptophanes: Design and Properties. In *Calixarenes and Beyond*; Neri, P., Sessler, J. L., Wang, M.-X., Eds.; Springer International Publishing: Cham, 2016; pp 525−557.

(31) (a) Caravan, P.; Ellison, J. J.; McMurry, T. J.; Lauffer, R. B. Gadolinium(III) Chelates as MRI Contrast Agents: Structure, Dynamics, and Applications. *Chem. Rev.* **1999**, *99*, 2293−2352. (b) Cacheris, W. P.; Quay, S. C.; Rocklage, S. M. The Relationship between Thermodynamics and the Toxicity of Gadolinium Complexes. *Magn. Reson. Imaging* **1990**, *8*, 467−481. (c) Caravan, P. Strategies for Increasing the Sensitivity of Gadolinium Based MRI Contrast Agents. *Chem. Soc. Rev.* **2006**, *35* (6), 512−523.

(32) (a) Bonnet, C. S.; Laine, S.; Buron, F.; Tircsó, G.; Pallier, A.; Helm, L.; Suzenet, F.; Tóth, É. A Pyridine-Based Ligand with Two Hydrazine Functions for Lanthanide Chelation: Remarkable Kinetic Inertness for a Linear, Bishydrated Complex. *Inorg. Chem.* **2015**, *54*, 5991−6003. (b) Winter, M. B.; Klemm, P. J.; Phillips-Piro, C. M.; Raymond, K. N.; Marletta, M. A. Porphyrin-Substituted H-NOX Proteins as High-Relaxivity MRI Contrast Agents. *Inorg. Chem.* **2013**, *52*, 2277−2279. (c) Garimella, P. D.; Datta, A.; Romanini, D. W.; Raymond, K. N.; Francis, M. B. Multivalent, High-Relaxivity MRI Contrast Agents Using Rigid Cysteine-Reactive Gadolinium Complexes. *J. Am. Chem. Soc.* **2011**, *133*, 14704−14709. (d) Datta, A.; Raymond, K. N. Gd−Hydroxypyridinone (HOPO)-Based High-Relaxivity Magnetic Resonance Imaging (MRI) Contrast Agents. *Acc. Chem. Res.* **2009**, *42*, 938−947. (e) Jocher, C. J.; Moore, E. G.; Xu, J.; Avedano, S.; Botta, M.; Aime, S.; Raymond, K. N. 1,2-Hydroxypyridonates as Contrast Agents for Magnetic Resonance Imaging: TREN-1,2-HOPO. *Inorg. Chem.* **2007**, *46*, 9182−9191. (f) Werner, E. J.; Avedano, S.; Botta, M.; Hay, B. P.; Moore, E. G.; Aime, S.; Raymond, K. N. Highly Soluble Tris-Hydroxypyridonate Gd(III) Complexes with Increased Hydration Number, Fast Water Exchange, Slow Electronic Relaxation, and High Relaxivity. *J. Am. Chem. Soc.* **2007**, *129*, 1870−1871.

(33) (a) Moula Karimdjy, M.; Tallec, G.; Fries, P. H.; Imbert, D.; Mazzanti, M. Confinement of a Tris-Aqua Gd(III) Complex in Silica Nanoparticles Leads to High Stability and High Relaxivity and Supresses Anion Binding. *Chem. Commun.* **2015**, *51*, 6836−6838. (b) Wartenberg, N.; Fries, P.; Raccurt, O.; Guillermo, A.; Imbert, D.; Mazzanti, M. A Gadolinium Complex Confined in Silica Nanoparticles as a Highly Efficient T_1/T_2 MRI Contrast Agent. *Chem. - Eur. J.* **2013**, *19*, 6980−6983. (c) Aime, S.; Castelli, D. D.; Crich, S. G.; Gianolio, E.; Terreno, E. Pushing the Sensitivity Envelope of Lanthanide-Based Magnetic Resonance Imaging (MRI) Contrast Agents for Molecular Imaging Applications. *Acc. Chem. Res.* **2009**, *42*, 822−831. (d) Platas-Iglesias, C.; Vander Elst, L.; Zhou, W.; Muller, R. N.; Geraldes, C. F. G. C.; Maschmeyer, T.; Peters, J. A. Zeolite GdNaY Nanoparticles with Very High Relaxivity for Application as Contrast Agents in Magnetic Resonance Imaging. *Chem. - Eur. J.* **2002**, *8*, 5121−5131. (e) Aime, S.; Frullano, L.; Geninatti Crich, S. G. Compartmentalization of a Gadolinium Complex in the Apoferritin Cavity: A Route To Obtain High Relaxivity Contrast Agents for Magnetic Resonance Imaging. *Angew. Chem., Int. Ed.* **2002**, *41*, 1017−1019. (f) Ananta, J. S.; Godin, B.; Sethi, R.; Moriggi, L.; Liu, X.; Serda, R. E.; Krishnamurthy, R.; Muthupillai, R.; Bolskar, R. D.; Helm, L.; et al. Geometrical Confinement of Gadolinium-Based Contrast Agents in Nanoporous Particles Enhances T_1 Contrast. *Nat. Nanotechnol.* **2010**, *5*, 815. (g) Courant, T.; Roullin, V. G.; Cadiou, C.; Callewaert, M.; Andry, M. C.; Portefaix, C.; Hoeffel, C.; de Goltstein, M. C.; Port, M.; Laurent, S.; et al. Hydrogels Incorporating GdDOTA: Towards Highly Efficient Dual T_1/T_2 MRI Contrast Agents. *Angew. Chem., Int. Ed.* **2012**, *51*, 9119−9122. (i) Sethi, R.; Ananta, J. S.; Karmonik, C.; Zhong, M.; Fung, S. H.; Liu, X.; Li, K.; Ferrari, M.; Wilson, L. J.; Decuzzi, P. Enhanced MRI Relaxivity of Gd^{3+}-Based Contrast Agents Geometrically Confined within Porous Nanoconstructs. *Contrast Media Mol. Imaging* **2012**, *7*, 501−508.

(34) Aime, S.; Botta, M.; Terreno, E. *Gd(III)-Based Contrast Agents for MRI*; Advances in Inorganic Chemistry, Vol. *57*; Elsevier, 2005; pp 173−237; .